

Valence transitions of Sm in monosulfide solid solutions

L. J. Tao and F. Holtzberg

IBM Thomas J. Watson Research Center, Yorktown Heights, New York 10598

(Received 6 August 1974)

Magnetic-susceptibility and lattice-parameter measurements indicate that Sm in $\text{Sm}_{1-x}\text{Y}_x\text{S}$ for $x > 0.15$, in $\text{Sm}_{1-x}\text{La}_x\text{S}$ for $x > 0.33$, and in $\text{Sm}_{1-x}\text{Gd}_x\text{S}$ for $x > 0.17$ is in an intermediate valence state at $T = 295$ K. A transition from this intermediate valence state to a more divalent but still intermediate valence state is observed on cooling and on heating from room temperature in $\text{Sm}_{1-x}\text{Y}_x\text{S}$ for $0.15 < x < 0.27$. For $x > 0.47$, Sm remains intermediate valent on cooling to $T = 4.2$ K and on heating to $T = 900$ K. Its susceptibility is independent of temperature below $T = 100$ K. Related effects are observed in the $\text{Sm}_{1-x}\text{La}_x\text{S}$ and in the $\text{Sm}_{1-x}\text{Gd}_x\text{S}$ systems. A model of interconfiguration fluctuations including multiple energy levels in both configurations and crystal-field effect may explain these results.

INTRODUCTION

Sm is a rare-earth element which can exist in either the divalent or the trivalent state in different compounds. The magnetic properties of the two states are quite different. Sm^{2+} with $4f^6$ configuration has a $J = 0$ ground state and shows temperature-independent Van Vleck susceptibility at low temperatures ($T < 100$ K).¹ Sm^{3+} with $4f^6$ configuration has a $J = \frac{5}{2}$ ground state and at low temperatures its susceptibility increases with decreasing temperature approximately according to Curie's law² and in some compounds it orders magnetically.³ Since the difference of the absolute values of the susceptibility and their temperature dependence in the two states are quite large, the valence state of Sm can be monitored by susceptibility measurements.

Sm in SmS is divalent and the compound is a black-colored semiconductor. It has been found to undergo a first-order semiconductor-to-metal transition at 6.5 kbar at 295 K.⁴ A large decrease in volume accompanies the transition but the NaCl structure is retained. From lattice-parameter and high-temperature (100–300 K) susceptibility measurements it is estimated that the collapsed metallic SmS has an intermediate valence of about 2.7.⁵ The susceptibility, however, shows neither Curie-like behavior nor ordering at low temperature ($T < 100$ K). Rather, its temperature dependence still resembles that of a Van Vleck ion with a constant susceptibility, but greatly suppressed in magnitude.

Recently, it has been shown that the effect of pressure on SmS can also be achieved by lattice compression in $\text{Sm}_{1-x}\text{La}_x\text{S}$, $\text{Sm}_{1-x}\text{Y}_x\text{S}$, $\text{Sm}_{1-x}\text{Gd}_x\text{S}$, and $\text{SmS}_{1-x}\text{As}_x$ systems,^{6,7} using the fact that LaS, YS, GdS, and SmAs (where Sm is trivalent) have smaller trivalent cationic radii than the Sm^{2+} . Further, a change of valence accompanied by explosive disintegration has been observed in some $\text{Sm}_{1-x}\text{Gd}_x\text{S}$

and $\text{SmS}_{1-x}\text{As}_x$ samples on cooling.^{6,7} In this paper we report the results on susceptibility and lattice-parameter measurements of the $\text{Sm}_{1-x}\text{Y}_x\text{S}$ and the $\text{Sm}_{1-x}\text{La}_x\text{S}$ systems for $0 \leq x \leq 1$. Temperature-induced change of valence with and without disintegration for different ranges of x are observed. Note that Y and La are nonmagnetic so that the magnetic properties of Sm in the intermediate valence state as well as its temperature dependence can be measured directly in these two systems. We have also extended the susceptibility measurement of the $\text{Sm}_{1-x}\text{Gd}_x\text{S}$ system to higher temperatures (900 K).

EXPERIMENTAL RESULTS

A Lattice parameter

Figure 1(a) shows the results of lattice-parameter measurements of $\text{Sm}_{1-x}\text{Y}_x\text{S}$ at $T = 295$ K and at $T = 80$ K as a function of x . A discontinuity is found to exist at $x \cong 0.15$ at $T = 295$ K. Samples with $x \leq 0.15$ are black colored and resemble undoped SmS. The lattice parameter contracts on cooling as expected. Samples with $x \geq 0.15$ are gold colored and their lattice parameters are substantially smaller than the linear interpolation between SmS and YS, indicating that Sm may have a mixed valence between 2 and 3. The valence can be estimated by taking the values 5.966 and 5.62 Å for pure divalent and trivalent SmS, respectively,⁶ and is shown in Fig. 1(b). In addition, the lattice parameter of these samples, in particular those near the discontinuity, expands on cooling and on heating from room temperature.

The temperature dependence of the lattice parameters of two samples with composition $\text{Sm}_{0.81}\text{Y}_{0.19}\text{S}$ and $\text{Sm}_{0.77}\text{Y}_{0.23}\text{S}$ obtained on single crystals is shown in Fig. 2.⁸ The crystals expand and their color changes from gold to black at $T \cong 185$ K and at $T \cong 160$ K, respectively. The NaCl crystal structure, however, is retained. The transition is reversible on warming and no appreciable hysteresis

is noted.

The temperature dependence of lattice parameter and color of samples with composition $\text{Sm}_{0.85}\text{Y}_{0.15}\text{S}$ is more complicated. At $T \cong 295$ K, single crystals as grown are gold colored with a lattice parameter of 5.69 Å (Fig. 1). The crystals expand, disintegrate, and change to black color on cooling over a range of $260 \gtrsim T \gtrsim 180$ K. At $T \cong 180$ K, the samples have completely disintegrated to a black powder with particle size of about 10 μm with a lattice parameter of 5.82 Å. However, the NaCl crystal structure is still retained. Further cooling does not cause further expansion. On warming, the powder remains black colored with the same lattice parameter of 5.82 Å up to room temperature and is stable. This is shown in Fig. 1 by the two values of lattice parameter (5.69 Å, gold and 5.82 Å, black colored) at one temperature (295 K) for $x = 0.15$. The black powder gradually changes to gold color at $T \cong 420$ K and remains gold colored on cooling to 295 K.

If we heat the samples with $0.15 \leq x \leq 0.23$ above room temperature, their color change again from gold to black gradually over a wide temperature range from 600 to 900 K. Preliminary lattice-parameter measurements indicate that the crystals also expand on heating to above 600 K.⁹

Samples with $x = 0.27$ show a smaller change in color and lattice parameter at even a lower temperature and a higher temperature than samples with smaller x . Samples with higher Y doping than $x = 0.47$ remain gold colored on cooling to $T \cong 80$ K and on heating to 600 K.

We have previously suggested⁶ that the explosive transformation is a consequence of concentration fluctuations in the sample. Regions of different

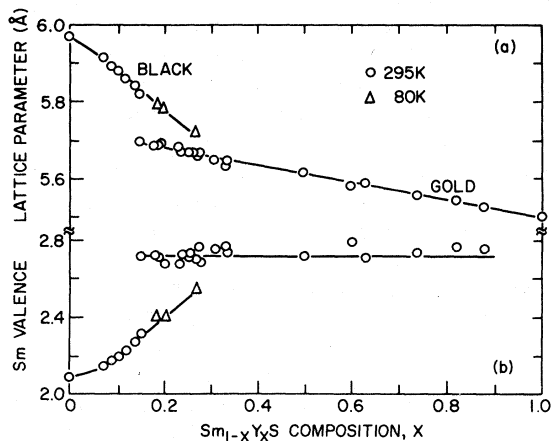


FIG. 1. (a) Lattice parameter, (b) Sm valence vs composition x for the $\text{Sm}_{1-x}\text{Y}_x\text{S}$ system. The valence of Sm in SmS (2.0–2.1) depends on the estimate of lattice parameter (5.955–6.00 Å) for ideally divalent SmS.

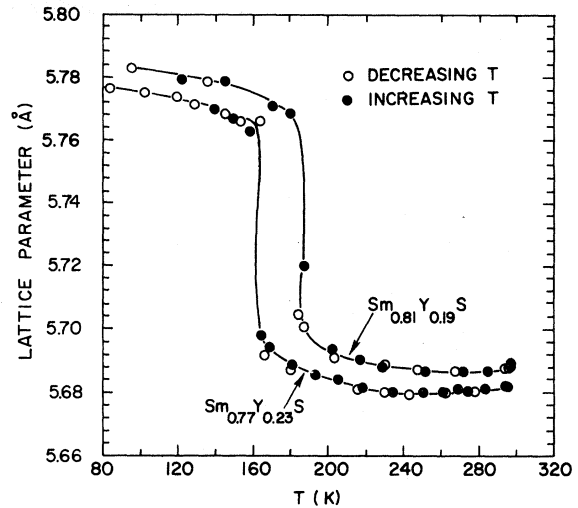


FIG. 2. Variation of lattice parameter with temperature for two single crystals with the composition $\text{Sm}_{0.77}\text{Y}_{0.23}\text{S}$ and $\text{Sm}_{0.81}\text{Y}_{0.19}\text{S}$. Black dots show data obtained on cooling, white circles on warming the crystal. The crystals are gold colored above their respective transition temperatures and black colored below.

compositions undergo phase transition at different temperatures and therefore expand at different temperatures. Differential stresses will be created among these regions. Furthermore, the closer the composition (as determined by electron microprobe analysis) to the discontinuity, the larger the expansion will be at low temperatures. Therefore, the stresses will be the largest for samples with x nearest to 0.15 at the transition temperature. The observations reported here supports this interpretation.

No discontinuity seems to exist in the $\text{Sm}_{1-x}\text{La}_x\text{S}$ system at room temperature. Samples with $x = 0.33$, however, contract only slightly, whereas samples with $x = 0.39$ expand on cooling and on heating. Their color changes from gold to dark brown at $T \cong 80$ K and at $T \cong 600$ K, indicating that these samples have similar characteristics to the gold phase samples of the $\text{Sm}_{1-x}\text{Y}_x\text{S}$ system. In the $\text{Sm}_{1-x}\text{Gd}_x\text{S}$ system, results similar to those of the $\text{Sm}_{1-x}\text{Y}_x\text{S}$ system are observed, with a discontinuity at $x \cong 0.16$.

B Magnetic susceptibility

The magnetic susceptibilities were measured by the Faraday method. The susceptibility in units of emu per mole of SmS is plotted in Figs. 3 and 4, respectively, for the $\text{Sm}_{1-x}\text{Y}_x\text{S}$ and $\text{Sm}_{1-x}\text{La}_x\text{S}$ systems for several values of x . For comparison, the susceptibility of Pd_3Sm with trivalent Sm ion is also plotted. Susceptibility of YS and LaS which were used as the starting materials were also measured. At low temperatures, their susceptibilities were

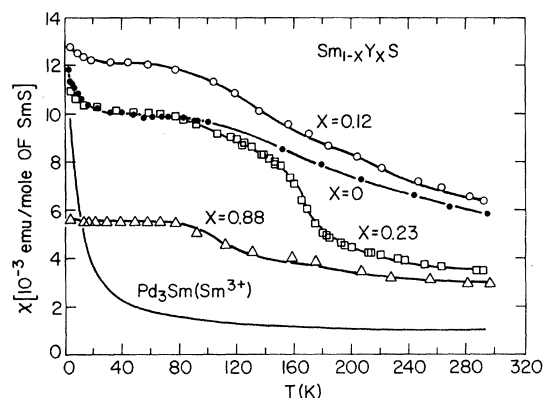


FIG. 3. Magnetic susceptibility vs temperature for three samples in the $\text{Sm}_{1-x}\text{Y}_x\text{S}$ system compared with SmS where Sm is divalent and with Pd_3Sm where Sm is trivalent.

found to be approximately inversely proportional to T . Since both La and Y are nonmagnetic, the Curie-like behavior is attributed to magnetic impurities in La and in Y . The part of susceptibility due to the impurities in La and Y as well as the small Pauli susceptibility of LaS and YS were subtracted proportionately from the measured susceptibility of $\text{Sm}_{1-x}\text{La}_x\text{S}$ and of $\text{Sm}_{1-x}\text{Y}_x\text{S}$. In so doing we have assumed that proportionately the same amount of impurities in LaS and YS are in the $\text{Sm}_{1-x}\text{La}_x\text{S}$ and $\text{Sm}_{1-x}\text{Y}_x\text{S}$ system. There are also trace magnetic impurities in Sm used as starting material. These impurities will still cause a small rise in susceptibility at the lowest temperature, as seen in Figs. 3 and 4. For clarity, the result for $\text{Sm}_{0.85}\text{Y}_{0.15}\text{S}$ is shown separately in Fig. 5. We will discuss the results for the $\text{Sm}_{1-x}\text{Y}_x\text{S}$ system first.

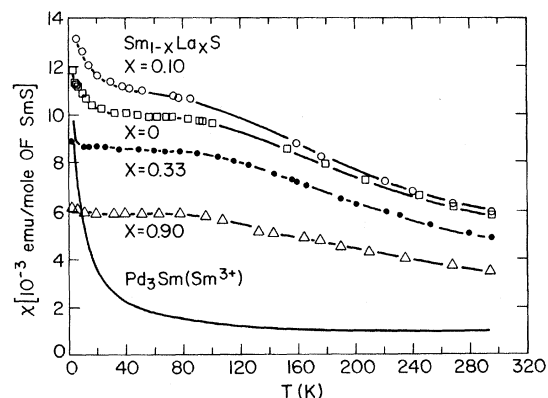


FIG. 4. Magnetic susceptibility vs temperature for three samples in the $\text{Sm}_{1-x}\text{La}_x\text{S}$ system compared with SmS where Sm is divalent and with Pd_3Sm where Sm is trivalent.

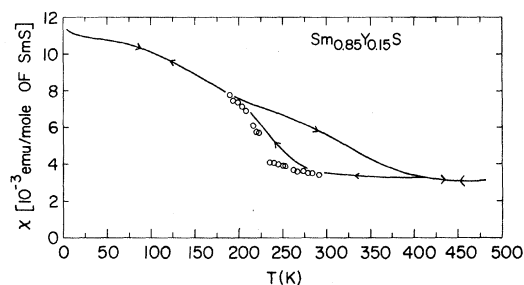


FIG. 5. Magnetic susceptibility vs temperature for a sample $\text{Sm}_{0.85}\text{Y}_{0.15}\text{S}$. White circles are data obtained on cooling single crystals for the first time from room temperature. Sudden jumps in susceptibility are associated with the explosive disintegration of the crystals. Lines are data from powdered sample (obtained by cooling single crystals). Arrows indicate warming or cooling cycles.

There are three major features to notice in Figs. 3 and 5. Firstly, the room-temperature susceptibility of the gold-phase samples have a value intermediate between those of Sm^{2+} and Sm^{3+} . It can be described by

$$\chi = \epsilon \chi_{\text{Sm}^{3+}} + (1 - \epsilon) \chi_{\text{Sm}^{2+}}, \quad (1)$$

where $\chi_{\text{Sm}^{3+}}$ and $\chi_{\text{Sm}^{2+}}$ are the susceptibility of Pd_3Sm and SmS , respectively, and $2 + \epsilon$ determine approximately the average valence of Sm in this phase.

Secondly, samples with $x \approx 0.15$ which show explosive disintegration on cooling between 260 and 180 K, also show discontinuous jumps in susceptibility, when cooled for the first time from single crystals as shown in Fig. 5. Below 180 K, the value of susceptibility is close to that of Sm^{2+} . On warming, a large thermal hysteresis is observed. At room temperature, the susceptibility is consistent with that of a divalent Sm . An intermediate value of susceptibility is again obtained at room temperature after the sample has been heated to about $T \approx 420$ K. These results are consistent with the temperature dependence of the color change and the lattice-parameter measurements described earlier. Repeated cooling and warming of powdered sample (obtained by cooling crystals) show a smoother transition with a large thermal hysteresis of about 200 deg.

Samples with $x \approx 0.23$ show a similar transition at a lower temperature at $T \approx 160$ K (Fig. 3). No appreciable thermal hysteresis is noted, consistent with the lattice-parameter measurements. The transition observed by susceptibility measurement is, however, much broader than that observed by lattice parameter measurement shown in Fig. 2. In general, about 50 mg of sample were used for susceptibility measurements. A single crystal of the order of only 10 μg was used for x-ray diffrac-

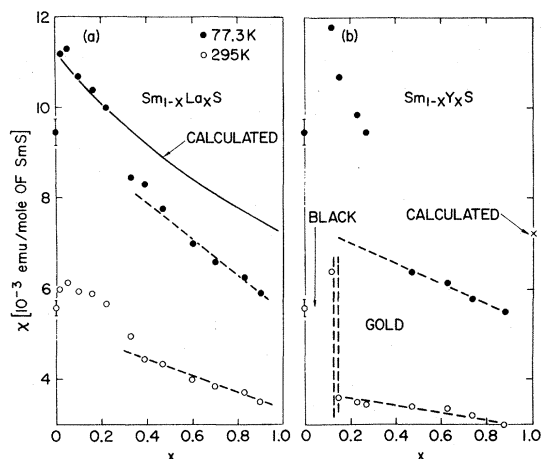


FIG. 6. Magnetic susceptibility vs composition x for $\text{Sm}_{1-x}\text{La}_x\text{S}$ (a) and for $\text{Sm}_{1-x}\text{Y}_x\text{S}$ (b) for two temperatures. Solid line in Fig. 6(a) is calculated assuming that Sm is divalent with exchange interaction between Sm ions taken account of. The dotted vertical lines in Fig. 6(b) separate the $\text{Sm}_{1-x}\text{Y}_x\text{S}$ system into black phase for $x < 0.12$ and gold phase for $x > 0.15$ at room temperature.

tion measurement to obtain the lattice parameter. Fluctuations of composition across a crystal will smear out a sharp transition in susceptibility. These fluctuations in composition are probably also responsible for the transition over a wide range of temperature observed in the $\text{Sm}_{0.85}\text{Y}_{0.15}\text{S}$ samples.

Thirdly, the susceptibility of gold-phase samples which do not show an expansion in their lattice parameter at low temperatures have a temperature-independent susceptibility below $T < 100$ K. The susceptibility does not increase as temperature decreases, as might be expected from the ϵ fraction of Sm^{3+} in the sample, estimated from room-temperature susceptibility. Furthermore, the value of susceptibility is not only smaller than that of undoped SmS, but is also smaller than the minimum possible value for a Sm^{2+} ion without any exchange enhancement, as will be discussed below. These facts are further evidence that Sm in these sample is in a state similar to that of collapsed SmS under pressure.⁵

Figure 4 shows similar effects observed in the $\text{Sm}_{1-x}\text{La}_x\text{S}$ system. A smaller transition toward more divalent-like Sm is seen in the susceptibility measurements in samples with $x \approx 0.33$ and $x \approx 0.39$ which show either small decrease or expansion of the lattice on cooling.

To see the effect of La and Y doping on the magnetic properties of Sm more clearly, we plotted the susceptibilities of $\text{Sm}_{1-x}\text{La}_x\text{S}$ and $\text{Sm}_{1-x}\text{Y}_x\text{S}$ for two temperatures as a function of x in Fig. 6. The two temperatures are 295 and 77.3 K, at which the susceptibility becomes independent or almost in-

dependent of temperature.

The susceptibility of undoped SmS varies from sample to sample, presumably due to nonstoichiometry (hence different degree of exchange enhancement between Sm ions, see below). This is the source of the error bar for the susceptibility of undoped SmS in Fig. 6.

We will first discuss the case of $\text{Sm}_{1-x}\text{La}_x\text{S}$ [Fig. 6(a)]. The initial increase of susceptibility with doping, at both high and low temperatures, has been interpreted as a result of enhancement of exchange interaction J between the Sm^{2+} ions due to the introduction of electrons into the conduction band from La doping.^{1,10} The solid curve in Fig. 6(a) is the calculated Van Vleck susceptibility as a function of x taking into account both the enhanced exchange between Sm^{2+} ions and the dilution effect due to La doping.¹⁰ The value of $\chi = 7.23 \times 10^{-3}$ (emu/mole of Sm) at $x = 1$ corresponds to the low-temperature susceptibility of a mole of Sm^{2+} ion in the absence of any exchange interaction. The susceptibility of samples with $x \leq 0.22$ falls on the calculated curve, confirming previous results. But for samples with $x \gtrsim 0.33$, the susceptibility falls considerably below the curve. Indeed, the susceptibility of a sample with $x \approx 0.90$ is about 20% smaller than the theoretically calculated minimum possible value for Sm^{2+} .

The general behavior of the $\text{Sm}_{1-x}\text{Y}_x\text{S}$ system, as shown in Fig. 6(b), is similar to but more dramatic than that of the $\text{Sm}_{1-x}\text{La}_x\text{S}$ system. The dashed lines at $x = 0.12$ and $x = 0.15$ divide the system into black and gold phases at room temperature. The susceptibility of all gold-phase samples varies smoothly and linearly with x at $T = 295$ K. At $T = 77.3$ K, however, the susceptibilities of the three samples with $0.15 \leq x \leq 0.27$ deviate from the extrapolation and have values closer to that of Sm^{2+} .

The magnetic-susceptibility measurement of $\text{Sm}_{1-x}\text{Gd}_x\text{S}$ from 4.2 to 300 K was previously reported by Jayaraman *et al.*⁷ A sudden increase in susceptibility at low temperatures corresponding to a valence transition of Sm was observed in samples with $0.16 \leq x \leq 0.22$. We have extended the measurement to higher temperatures ($T = 900$ K). We observed a discontinuity in the $\text{Sm}_{1-x}\text{Gd}_x\text{S}$ system at $x \approx 0.17$ similar to the $\text{Sm}_{1-x}\text{Y}_x\text{S}$ system. The reciprocal susceptibility of a gold-phase sample (gold colored at room temperature) $\text{Sm}_{0.85}\text{Gd}_{0.17}\text{S}$ and of a black-phase sample $\text{Sm}_{0.85}\text{Gd}_{0.15}\text{S}$ is plotted in Fig. 7 as a function of temperature. At room temperature, the susceptibility of the gold-colored sample $\text{Sm}_{0.85}\text{Gd}_{0.17}\text{S}$ is smaller than that of the black phase sample $\text{Sm}_{0.85}\text{Gd}_{0.15}\text{S}$ (i. e., $1/\chi$ is larger in the gold phase). At both low and high temperatures, when the sample $\text{Sm}_{0.85}\text{Gd}_{0.17}\text{S}$ changes its color from gold to black, the susceptibility also approaches that of the black-phase sample.

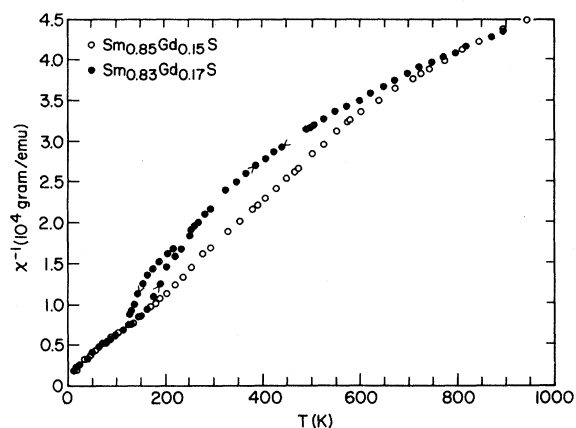


FIG. 7. Reciprocal susceptibility of two samples $\text{Sm}_{1-x}\text{Gd}_x\text{S}$ at $x=0.15$ and at $x=0.17$, respectively, vs temperature. The sample at $x=0.15$ is black colored at all temperatures while the sample at $x=0.17$ is black colored for $T > 600$ K and for $T \lesssim 250$ K but gold colored in between. Note that when the sample at $x=0.17$ changes color from gold to black at both high and low temperature, its susceptibility also approaches to that of the black colored sample at $x=0.15$.

The susceptibility of the two samples in both phases is dominated by the Gd ions, in particular at low temperatures ($T \lesssim 600$ K). It can be approximately described by the Curie-Weiss law

$$\chi = C/(T - \theta) = C/(T + |\theta|), \quad (2)$$

where θ is negative (antiferromagnetic-exchange interaction). An increase of lattice parameter of the sample $\text{Sm}_{0.83}\text{Gd}_{0.17}\text{S}$ at low and at high temperatures reduce the exchange interaction between the Gd ions and decrease the absolute magnitude of θ . This decrease of θ , from Eq. (2), will increase χ or decrease $1/\chi$, as observed.

A T - x phase diagram can be constructed for the three system. One such diagram for the $\text{Sm}_{1-x}\text{Y}_x\text{S}$ system is sketched in Fig. 8. The transition temperature from the G phase to the B phase decreases as x (Y doping) increases, as indicated by the G - B boundary. The change in color, in lattice parameter, and in susceptibility between the G and the B phases becomes less and less prominent as x increases and for $x \geq 0.47$, a transition is not detected in our measurements. The boundary between G and B phases at high temperature is not well defined. The slashed region indicates that this is a broader transition in contrast to the sharp transition at low temperatures.

DISCUSSION

The unusual behavior of Sm in the gold-phase samples of $\text{Sm}_{1-x}\text{La}_x\text{S}$, $\text{Sm}_{1-x}\text{Y}_x\text{S}$, and $\text{Sm}_{1-x}\text{Gd}_x\text{S}$ and in the collapsed phase of SmS under pressure

is not unique among rare-earth metals and their compounds. SmB_6 , Ce metal, Ce, and Yb in some intermetallic compounds also have an intermediate valence.¹¹ Although one of the neighboring valence state (Ce^{3+} , Sm^{3+} , and Yb^{3+}) is magnetic, these materials with intermediate valence do not show Curie-like susceptibility at low temperatures, suggesting that the ground state of the intermediate valence state is nonmagnetic.

To interpret the nonmagnetic ground state of Sm in SmB_6 , Nickerson *et al.*¹² proposed that Sm ions on equivalent sites can exist in either the $4f^6$ or the $4f^5(5d-6s)$ configurations. The ground state of $4f^5(5d-6s)$ can be constructed to have $g_J = 0$ and thus no magnetic moment.¹² This model of non-homogeneous spatial mixture was rejected by Maple and Wohleben¹¹ on grounds that it is unphysical and that no two phase regions are detected in x-ray diffractions of carefully prepared samples in the intermediate valence state. Instead they suggested^{5,11} a temporal mixture of $4f^5$ and $4f^6$ configurations for a single Sm ion, based on an inter-configuration-fluctuation model (ICF) first introduced by Hirst.¹³ It is a state where the $4f^5$ and the $4f^6$ energy levels are degenerate within certain widths and are tied at the Fermi level. The Sm ion switches from one integral valence state ($2+$) with six local electrons on the $4f$ shell to the other state ($3+$) with five electrons on the $4f$ shell and with the extra electron in the conduction band. At high temperatures the susceptibility is the average of those of the two configurations. But at temperatures lower than the fluctuation temperature $T_f \lesssim \Delta/k_B$, where Δ is the energy width of the states of the two configurations, magnetic ordering or divergence of susceptibility is prevented due to the incoherent emission and reabsorption process.

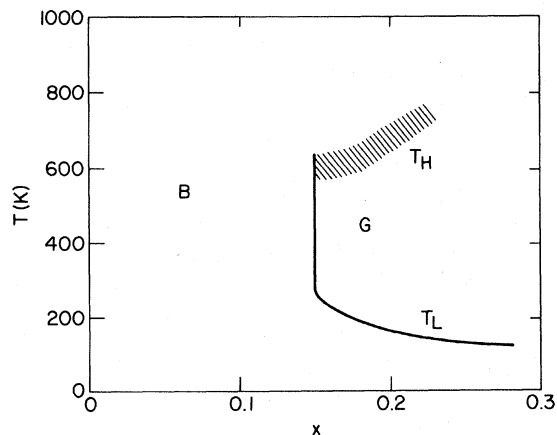


FIG. 8. T vs x phase diagram for $\text{Sm}_{1-x}\text{Y}_x\text{S}$. B indicates that samples are black colored in those regions while G indicates gold color in that region.

The idea of fluctuating between two valence states can also be applied to the model of Nickerson *et al.*, i. e., the Sm ion is switching between $4f^6$ ($J=0$) state and $4f^5(5d-6s)$ ($J=3$, but $g_J=0$) state. Since both states have zero magnetic moment, the time average of the two naturally has a vanishing magnetic moment. There are, however, more fundamental differences between the two models. In order to apply the model of Nickerson *et al.* to other intermediate valent rare earths, different rare-earth ions have to be treated differently to construct a ground-state wave function. It may for example lead to difficulties in explaining the case of nonmagnetic Ce which in this model will fluctuate between $4f^1$ and $(5d-6s)$ configurations, since $4f^1$ configuration has a magnetic $J=\frac{5}{2}$ ground state. It will also predict a magnetic ground state for Eu in EuCu_2Si_2 compound where Eu is fluctuating between $4f^6(5d-6s)$ and $4f^7$ ($S=\frac{7}{2}$) configurations.¹⁴ The ICF model suggested by Maple and Wohleben will in general predict a nonmagnetic ground state at low temperatures regardless of the details of the configurations. In this respect, a study of the magnetic properties of EuCu_2Si_2 to see if the intermediate valent Eu in this compound is magnetic or not at low temperature can be very important.

The nonmagnetic state at low temperatures in the ICF model can be more easily understood in the following way. The $J=\frac{5}{2}$ state of $4f^5$ configuration will split into six Zeeman levels in a magnetic field. The Curie susceptibility ($\chi \propto 1/T$) is a result of the Boltzmann distribution among the Zeeman levels. When a Sm ion changes from $4f^6$ configuration to $4f^5$ configuration, it can occupy any one of the six Zeeman levels. This is possible because the energy involved in emitting and absorbing an electron is much larger than the energy separations between the Zeeman levels. If it goes into a high Zeeman level it will relax to the lower levels at low temperatures to achieve a proper Boltzmann distribution. A fast transition back to the other configuration ($4f^6$), however, will prevent the thermal equilibrium moment from developing in the $4f^5$ configuration.

The temperature-induced transitions between the valence states of Sm ion can be understood within the framework of the ICF model, taking into considerations the multiple energy levels in both configurations and the crystal-field effect on Sm ions in $4f^5$ configuration and on the d conduction band. A schematic diagram of proposed energy levels as a function of temperature for the B and G phases (see Fig. 8) for a particular composition is plotted in Fig. 9. T_L indicates the transition temperature between the G and B phases on cooling, whereas T_H indicates the beginning of a transition from G to B phase on heating. Note that the meaning of the energy diagram shown in Fig. 9 differs somewhat

from the one usually used. As discussed above, in the ICF model, a Sm ion at any one moment occupies a state in either the f^6 or the f^5d configurations. In the f^5d configuration, the ground state $J=\frac{5}{2}$ of the five f electrons splits into a Γ_7 doublet and a Γ_8 quartet. Assuming the crystal-field parameters have the same signs and order of magnitude as those in other metallic rare-earth sulfides,¹⁵ Γ_7 is the ground state and the energy separation between Γ_7 and Γ_8 is less than 100 K. The energy level of the conduction band is not shown in Fig. 9. The cubic crystal field will also split the d band into e_g and t_{2g} two branches. The Fermi level of the lower branch of the d band is presumably tied with the $J=\frac{5}{2}$ level of the f^5 configuration. Further, all the levels are broadened due to the fluctuations. Figure 9, however, only shows the change of the center of the average energy levels in the two configurations in different phases as a function of temperature.

We shall now attempt to suggest a mechanism for the temperature-induced transitions. In Fig. 9 at $T \gg T_H$ where the system is well in the B phase, all the levels shown in Fig. 9 are populated at one instant or another as the Sm ion fluctuates between the two configurations. As the temperature lowers, the $J=1$ state becomes depopulated. The system may find at a certain temperature that its total en-

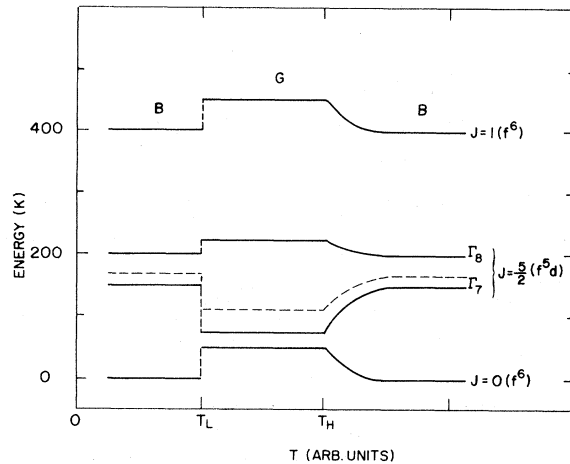


FIG. 9. Schematic energy level diagram as a function of temperature for a sample $\text{Sm}_{1-x}\text{R}_x\text{S}$, where $R=\text{Y}$, Gd , or La at a particular x . The Sm ion fluctuates between f^6 and f^5d configurations. The energy level of the d band is not shown. T_H and T_L indicate the two transition temperatures. Note that the energy levels of the trivalent state (with $J=\frac{5}{2}$ as the ground state) is relatively lower than those of the divalent state in the G phase, where lattice is contracted, than in the B phase. The crystal-field strength is also larger in the G phase since the lattice parameter is smaller. Therefore, the energy separation between the Γ_7 and Γ_8 states is larger in the G phase than in the B phase.

ergy can be lowered if the energy separation between the Γ_7 and Γ_8 levels is widened and the Γ_7 level is more populated relative to the Γ_8 level. The energy separation between the two levels can be increased if the crystal-field strength is increased. This in turn can be achieved by contraction of the lattice. In addition, the contraction of the lattice will lower the energy level of the trivalent state (f^5d) with respect to the divalent state (f^6). This is shown in Fig. 9 by raising the average of the $J=0$ and $J=1$ levels and lowering the average of Γ_7 and Γ_8 levels. At the same time, the lower branch of the d band will also be lowered together with the $J=\frac{5}{2}$ states as the separation between the e_g and t_{2g} branches widens as a result of the increase in crystal-field strength. These effects will further increase the population in the f^5d configuration and a spontaneous transition may result under favorable condition. As a consequence of this transition, the intermediate valence of Sm ions becomes more trivalent, the number of carriers increases, and the color of the samples changes to gold. An equilibrium will be reached at a temperature T_H and from there on the samples will remain gold as the temperature lowers. At an even lower temperature, however, the Γ_7 state will start to be depopulated and the system may find that its total energy can be lowered if the $J=0$ energy level of the state is lowered. This can be achieved by expansion of the lattice parameter back to the same value as that in the high-temperature B phase. As a result of the expansion, the crystal-field strength weakens, the energy levels of the lower branch of the d band and of the f^5 configuration increase relative to f^6 configuration. This will further populate the $J=0$ state and again, under certain conditions, a sharp spontaneous transition may occur (for example, the transitions of the two samples shown in Fig. 2) which returns the system to a more divalent state (B phase), decreases the number of carriers, and changes the color back to black.

The expansion of the lattice at both T_L and at T_H , however, will cost elastic energy, in particular on the part of the trivalent Y or other trivalent rare-earth dopings. This cost of elastic energy increases proportionally to the concentration of doping x . Therefore, for samples with x larger than a critical value, the system will remain in an intermediate valence state to below 80 and up to 900 K.

It is interesting to point out that an analogous phenomenon exists in cooperative Jahn-Teller phase transition. Here instead of contraction of lattice, a distortion of lattice to lower symmetry is involved

in the transition. Using molecular-field theory, Pytte and Stevens¹⁶ have predicted that for a certain range of parameters, there may exist two Jahn-Teller transition temperatures. The crystal distorts at the first transition temperature, but returns to its original symmetry at the second lower transition temperature. Indeed, this phenomena has recently been observed in the $Tb_{1-x}Gd_xVO_4$ system for a narrow range of x .¹⁷ The energy levels involved for the Tb ion is a doublet sandwiched in between two singlets. Note that this energy-level diagram is very similar to that of Sm ion in the intermediate valence state suggested in Fig. 9. The doublet of the Tb ion corresponds to the Γ_7 and Γ_8 states of the Sm ion while the two singlets correspond to the $J=0$ and the $J=1$ states. A distortion in the Jahn-Teller system splits the doublet of Tb^{3+} while a contraction in lattice widens the separation between Γ_7 and Γ_8 states of Sm^{3+} . In both systems, the elastic energy is also involved in calculating the total free energy.

CONCLUSION

We have demonstrated that as a result of lattice pressure, Sm in $Sm_{1-x}Y_xS$ for $x \gtrsim 0.15$, in $Sm_{1-x}La_xS$ for $x \gtrsim 0.33$, and in $Sm_{1-x}Gd_xS$ for $x \gtrsim 0.17$ is in an intermediate valence state at $T = 293$ K. A temperature-induced transition from this intermediate state to a more divalent state is observed on cooling and on heating in $Sm_{1-x}Y_xS$ for $0.15 \leq x \leq 0.27$. This transition is reversible. For $x \gtrsim 0.47$, Sm retains its intermediate valence on cooling and on heating. Its susceptibility is temperature independent for $T \lesssim 100$ K. Related effects are also observed in the $Sm_{1-x}La_xS$ and $Sm_{1-x}Gd_xS$ systems. We have shown that a model of interconfiguration fluctuations can explain the intermediate valence state observed in Sm and that in this model a Curie-like moment will not develop in the Sm^{3+} configuration ($4f^5$) but a Van Vleck moment is present in the Sm^{2+} configuration ($4f^6$). By introducing crystal-field effect and the dependence of its strength on the lattice parameter into the ICF model, we can qualitatively account for the temperature-induced transitions between valence states.

ACKNOWLEDGMENTS

We thank T. Penney, E. Pytte, J. Freeoff, M. Nathan, and J. Torrance for many helpful discussions; H. Lilienthal and P. Lockwood for technical assistance; and D. Wohlleben for a private correspondence. It is also a pleasure to acknowledge the help of R. Tournier in the early phases of this work.

¹J. B. Torrance, F. Holtzberg, and T. R. McGuire, AIP Conf. Proc. **10**, 1279 (1973).

²W. E. Gardner, J. Penfold, and I. R. Harris, J. Phys.

(Paris) Suppl. **32**, C1-1139 (1971).

³K. H. J. Buschow, H. W. deWijn, and A. M. van Diepen, Proceedings of the Seventh Rare Earth Research Con-

- ference, Coronado, Calif., 1968 (unpublished).
- ⁴A. Jayaraman, V. Narayanamurti, E. Bucher, and R. G. Maines, *Phys. Rev. Lett.* 25, 1430 (1970).
- ⁵M. B. Maple and D. Wohlleben, *Phys. Rev. Lett.* 27, 511 (1971).
- ⁶F. Holtzberg, *AIP Conf. Proc.* 18, 478 (1974).
- ⁷A. Jayaraman, E. Bucher, P. D. Dernier, and L. D. Longinotti, *Phys. Rev. Lett.* 31, 700 (1973).
- ⁸The data of Figs. 1 and 2 are somewhat different from the results obtained on old samples as previously reported in Ref. 6. The difference between the old and new samples is related to the cation/anion ratio. The old samples have a ratio near unity while the new samples have excess cations and transform explosively near the discontinuity.
- ⁹A. Jayaraman, P. Dernier, and L. D. Longinotti (report of work prior to publication).
- ¹⁰F. Mehran, J. B. Torrance, and F. Holtzberg, *Phys. Rev. B* 8, 1268 (1973).
- ¹¹See, for example, M. B. Maple and D. Wohlleben, *AIP Conf. Proc.* 18, 447 (1974).
- ¹²J. C. Nickerson, R. M. White, K. N. Lee, R. Bachmann, T. M. Geballe, and G. W. Hull, Jr., *Phys. Rev. B* 3, 2030 (1971).
- ¹³L. L. Hirst, *Phys. Kondens. Mater.* 11, 255 (1970).
- ¹⁴E. R. Bauminger, D. Froindlich, I. Nowik, S. Ofer, L. Felner, and I. Mayer, *Phys. Rev. Lett.* 30, 1053 (1973).
- ¹⁵L. J. Tao, J. B. Torrance, and F. Holtzberg, *Solid State Commun.* 15, 1025 (1974).
- ¹⁶E. Pytte and K. W. H. Stevens, *Phys. Rev. Lett.* 27, 862 (1971).
- ¹⁷R. T. Harley, W. Hayes, A. M. Perry, and S. R. P. Smith, *Solid State Commun.* 14, 521 (1974).